Sakarya Üniversitesi Fen Bilimleri Dergisi
Sakarya University Journal of Science

e-ISSN : 2147-835X
Publisher : Sakarya University

Vol. 29, No. 2, 151-159, 2025
DOI: https://doi.org/10.16984/saufenbilder.1615457

Research Article

# Lattice Boltzmann Modelling of Natural Convection Problems in a Cavity with a Different Wall Temperature

Erman Aslan[1*], Ozlem Yalcin[2]

[1] Kocaeli University, Faculty of Engineering, Department of Mechanical Engineering, Kocaeli, Türkiye, erman.aslan@kocaeli.edu.tr, ror.org/0411seq30
[2] Istanbul Gelişim University, Faculty of Engineering and Arhitecture, Department of Aeronautical, İstanbul, Türkiye, oyalcin@gelisim.edu.tr, ror.org/0188hvh39
*Corresponding Author

ARTICLE INFO

Keywords:
Lattice Boltzmann Method
Natural convection
Computational fluid dynamics
Laminar flow
Nusselt number

Article History:
Received: 07.01.2025
Revised: 03.03.2025
Accepted: 05.03.2025
Online Available: 15.04.2025

ABSTRACT

In this study, the cyclic natural convection problem in a square enclosure is modeled using the Lattice Boltzmann Method (LBM) under laminar flow conditions. Four different combinations of boundary conditions are employed to create cases. These cases are denoted as HHHC (Horizontal Hot Horizontal Cold), HHVC (Horizontal Hot Vertical Cold), VHHC (Vertical Hot Horizontal Cold), and VHVC (Vertical Hot Vertical Cold). Four Rayleigh numbers have been utilized to represent laminar flow conditions, namely $Ra$=$10^4$, $10^5$, $10^6$, and $10^7$. For validation purposes, the well-validated finite volume method-based commercial code Ansys-Fluent is employed. In the VHVC model and at the highest Rayleigh number, the results obtained with LBM were compared to and validated against the results obtained with the finite volume method. Nusselt numbers are compared for the four cases based on Rayleigh numbers, and the case with highest heat transfer identified. Cases of HHHC and VHVC have produced the lowest and highest Nusselt number, respectively.

## 1. Introduction

Numerical modeling of natural convection heat transfer for an enclosure has garnered significant attention. This modeling finds applications in various engineering fields such as building insulation, fire prevention systems, solar collectors, food preservation systems, compact heat exchangers, and cooling systems employed in electricity or nuclear power generation plants, among others [1, 2]. Our problem consists of three main subjects. Firstly, natural convection in a square enclosure; secondly, the Lattice Boltzmann Method; and finally, natural convection in a square enclosure with Lattice Boltzmann modeling; therefore, the literature review is divided into three parts.

Lage and Bejan [3] explored the numerical and theoretical aspects of natural convection resonance within an enclosure subjected to periodic heating from the side. One side was cold (constant temperature), the other side was heated with pulsating heat flux in a two-dimensional square enclosure. In the numerical computations, Prandtl number varied between 0.01 and 0.7, the heat flux Rayleigh number range was $10^3$-$10^9$, and nondimensional frequency range of 0-0.3 was applied. Theoretical considerations revealed that the numerically determined critical frequencies could be predicted by aligning the period of the pulsating heat input with the rotation period of the enclosed fluid. Mahdavi et al. conducted both experimental and numerical studies to investigate the thermal and hydrodynamic characteristics of laminar natural convective flow within a rectangular cavity filled with water and air [4].

The enclosure has a unique aspect ratio. Two vertical walls were applied to constant temperature boundary conditions with one wall

Cite as: E. Aslan, O. Yalcin (2025). Lattice Boltzmann Modelling of Natural Convection Problems in a Cavity with a Different Wall Temperature, *Sakarya University Journal of Science*, 29(2), 151-159. https://doi.org/10.16984/saufenbilder.1615457

being hot, the other cold. All other walls were properly insulated. The finite volume-based commercial code Ansys-Fluent was used for numerical investigations. The numerical results were in good agreement with measured data. The distortion of air is much higher than water. Ugurbilek et al. conducted a numerical investigation of three-dimensional natural convection in an air-filled cubical enclosure with gradually changing partitions [5]. The steady-state governing equations were resolved using the Boussinesq approximation and the finite volume method. Two scenarios were examined: one with partitions positioned perpendicularly (Case-1) and another with partitions positioned parallel (Case-2).

The opposing lateral walls of the enclosure were subjected to heating and cooling, while the remaining walls were considered adiabatic. Case-2 played major roles for convective heat transfer. Pesso and Piva investigated steady free convection at low Prandtl numbers numerically, which was caused by large density differences in a square cavity [6]. The Nusselt number was derived at Rayleigh numbers ranges of 10 and $10^8$, Prandtl number ranges of 0.0071 and 7.1, and Gay-Lussac number ranges of 0 and 2. Consequently, a Nusselt number correlation was proposed based on physical arguments. Numerical analysis of the natural convection phenomenon resulting from nonuniform wall heating in a square cavity was investigated at laminar Rayleigh numbers by Turkyilmazoglu [7]. A finite element technique was employed for the numerical simulation of thermally driven flow.

The best heat transfer rate was acquired as the heating took place near the top wall of the heated boundary. Turkyilmazoglu investigated a different type of lid-driven cavity flow in which the single lid is separated into two joint active/passive walls representing potential stirrers during a chemical mixing process [8]. The right portion of the wall is allowed to move freely to the right at a uniform velocity, while the left portion, attached to the adjacent wall at a point of dislocation, is regarded as stationary or able to move freely at a constant speed. A finite element approach was used to solve numerically.

The Lattice Boltzmann Method (LBM) offers an innovative numerical strategy for modeling viscous, incompressible flows within the subsonic range [9-14]. Instead of directly addressing the traditional continuum hydrodynamic equations, LBM aims to replicate fluid flow by monitoring the evolution of distribution functions of microscopic fluid particles. This kinetic characteristic of LBM introduces unique attributes that distinguish it from other numerical methods, including simplified modeling of fluid interactions and complete parallelism. In the last twenty years, LBM has garnered significant attention and interest, witnessed rapid progress in developing novel models and applications across diverse fields [9-11]. Although LBM has proven successful in simulating isothermal flow problems, its application in heat transfer systems has encountered challenges, primarily due to severe numerical instability in thermal models.

Karki et al. studied natural convection cavity numerically with different aspect ratios and using the lattice Boltzmann method [15]. The right side and left side walls were hot and cold, respectively, the other sides were adiabatic. Prandtl number kept constant at 0.71 and Rayleigh numbers varied between $10^3$ and $10^6$. The Nusselt number, streamlines and isotherms were observed to understand the physics of the problem. It was found that Nusselt number increases with Rayleigh number, and high aspect ratios have a negative effect on Nusselt number. Feng et al. introduced a novel thermal lattice Boltzmann (LB) model designed for numerically simulating natural convection under conditions characterized by significant temperature disparities and elevated Rayleigh numbers [16].

A regularization method was devised for the lattice Boltzmann equation, incorporating a third-order expansion of equilibrium distribution functions and introducing a temperature term to restore the equation of state for an ideal gas. Wei et al. developed a novel two-dimensional coupled lattice Boltzmann model via modified thermal equilibrium function for thermal incompressible fluid flows [17].
This novel numerical model gave more stability than standard lattice Boltzmann method. Present model was successfully assessed in free

convection cavity problem at laminar flow. Lattice Boltzmann analysis on natural convection heat transfer and fluid flow in a two-dimensional square enclosure with sinusoidal wave and different convection mechanism was investigated by Pichandi and Anbalagan [18].

In LBM analysis, single relaxation time (SRT) and D2Q9 lattice links was used. The working fluid was air ($Pr$=0.71). Nusselt number, isotherms and streamlines were observed to comprehend the physics of the problem. In recent years, the use of machine learning in natural convection problems within enclosed domain using LBM has been present [19]. Additionally, GPU parallel computing approaches [20] have also been employed for such problems

This study employs the Lattice Boltzmann Method (LBM) to model the cyclic natural convection problem within a square enclosure under laminar flow conditions. Four distinct combinations of boundary conditions, which are Horizontal Hot Horizontal Cold (HHHC), Horizontal Hot Vertical Cold (HHVC), Vertical Hot Horizontal Cold (VHHC) and Vertical Hot Vertical Cold (VHVC), are utilized to establish different cases. These cases are assessed with four Rayleigh numbers (Ra=$10^4$, $10^5$, $10^6$, and $10^7$) representing laminar flow conditions. Investigating natural convection heat transfer with four different Rayleigh numbers in laminar flow under four different boundary condition combinations and writing an in-house LBM code constitutes the originality of this study.

In order to validate our code and results, the well-validated finite volume method-based commercial code, Ansys-Fluent, is employed [21]. In the VHVC model, particularly, at the highest Rayleigh number, LBM results are compared and validated against those obtained using the finite volume method. Nusselt numbers are then compared across the four cases based on their respective Rayleigh numbers, enabling the identification of cases exhibiting the highest heat transfer.

### 1.1. Problem definition

Figure 1 shows the physical model of the present study. A two-dimensional natural convection within a square enclosure filled with air ($Pr$=0.71). Length and width of the domain are same. Four different Rayleigh numbers which includes laminar flow conditions have been considered, and these values are $Ra$=$10^4$, $10^5$, $10^6$ and $10^7$. Rayleigh number is based on length of domain. Gravitational acceleration ($g$) is imposed in negative y direction.

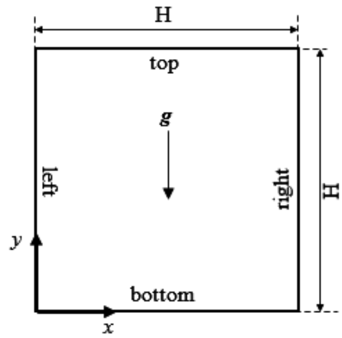


**Figure 1.** Physical model

In Table 1, four different cases with thermal boundary conditions are represented. The nondimensional temperature $\theta$ can range between zero and one, where $\theta$ equals 0 representing cold, and $\theta$ equals 1 representing hot. The first case is named HHHC, where the top wall and bottom wall are cold and hot, respectively, and the other walls are adiabatic ($q'' = 0$). The second case, HHVC, features a hot bottom wall and a cold left wall, with the other walls being adiabatic. In the third case, VHHC, the top wall and left walls are cold and hot, respectively, while the other walls remain adiabatic. Finally, the last case is VHVC, where the left wall is cold, the right wall is hot, and the other walls are adiabatic. All walls are stationary, and no-slip boundary conditions are applied for the momentum equation.

**Table 1.** Thermal boundary conditions

| Model | top | bottom | left | right |
|---|---|---|---|---|
| HHHC | $\theta = 0$ | $\theta = 1$ | $q'' = 0$ | $q'' = 0$ |
| HHVC | $q'' = 0$ | $\theta = 1$ | $\theta = 0$ | $q'' = 0$ |
| VHHC | $\theta = 0$ | $q'' = 0$ | $\theta = 1$ | $q'' = 0$ |
| VHVC | $q'' = 0$ | $q'' = 0$ | $\theta = 0$ | $\theta = 1$ |

### 1.2. LBM formulation

The LBM formulations most commonly utilizes rely on the single relaxation time approximation by Bhatnagar-Groos-Krook (BGK) [22]. In the present work, incompressible LBM formulation is adopted [23]. The two-dimensional and nine-velocity lattice model (D2Q9) shown in Figure 2 is used.

Based on current modeling, two distinct distribution functions are employed—one for density (momentum) and another for temperature (energy). The lattice Boltzmann evaluation equations for momentum and energy transport, discretized on a lattice, are typically addressed in two sequential steps: first, the "collision" step, followed by the subsequent "streaming" step.

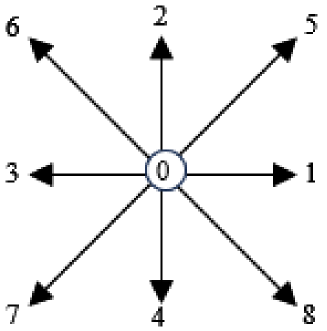

**Figure 2.** D2Q9 lattice model

- Collision

$$\tilde{f}_k(\vec{x},t+\delta t)=f_k(\vec{x},t)-\omega\left[f_k(\vec{x},t)-f_k^{eq}(\vec{x},t)\right]+F\delta t \quad (1a)$$

$$\tilde{g}_k(\vec{x},t+\delta t)=g_k(\vec{x},t)-\omega_T\left[g_k(\vec{x},t)-g_k^{eq}(\vec{x},t)\right] \quad (1b)$$

- Streaming

$$f_k(\vec{x}+\vec{c}_k\delta t,t+\delta t)=\tilde{f}_k(\vec{x},t+\delta t) \quad (2a)$$

$$g_k(\vec{x}+\vec{c}_k\delta t,t+\delta t)=\tilde{g}_k(\vec{x},t+\delta t) \quad (2b)$$

For natural convetion, external force ($F$) is defined via Boussinesq approximation. It is only applied in negative y direction due to gravitional accelaration.

$$F=\rho g\beta[T-T_{mean}] \quad (3)$$

where $\rho$ and $\beta$ are density and thermal expansion cofficient, respectively. $T$ represents the local air temperature at square domain, while $T_{mean}$ indicates the mean temperature of air. The collision frequencies are defined for momentum and energy equations as follows;

$$\omega=1/\left(\left(\frac{\nu}{c_s^2}\delta t\right)+0.5\right) \quad (4a)$$

$$\omega_T=1/\left(\left(\frac{\alpha}{c_s^2}\delta t\right)+0.5\right) \quad (4b)$$

Here, $\nu$ and $\alpha$ represents the kinematic viscosity and thermal diffusivity. And the lattice sound of speed $c_s$ and lattice speed $c$ are defined as:

$$c_s=c/\sqrt{3} \quad (5)$$

$$c=\delta/\delta t \quad (6)$$

The nine discrete velocities based on D2Q9 lattice model are:

$$\vec{c}_k=c\begin{bmatrix}0 & 1 & 0 & -1 & 0 & 1 & -1 & -1 & 1\\ 0 & 0 & 1 & 0 & -1 & 1 & 1 & -1 & -1\end{bmatrix} \quad (17)$$

The equilibrium distribution functions are for momentum and energy equations:

$$f_k^{eq}=w_k\rho\left[1+\frac{3}{c^2}\vec{c}_k\vec{u}+\frac{9}{2c^4}(\vec{c}_k\vec{u})^2-\frac{3}{2c^2}\vec{u}\vec{u}\right] \quad (8a)$$

$$g_k^{eq}=w_kT\left[1+\frac{3}{c^2}\vec{c}_k\vec{u}\right] \quad (8b)$$

with weighting foctors of D2Q9 lattice.

$$w_k=\begin{bmatrix}\frac{4}{9} & \frac{1}{9} & \frac{1}{9} & \frac{1}{9} & \frac{1}{9} & \frac{1}{36} & \frac{1}{36} & \frac{1}{36} & \frac{1}{36}\end{bmatrix} \quad (9)$$

The macroscopic (density, pressure, velocity and temperature) fields are obtained from:

$$\rho=\sum_{k=0}^{8}f_k=\sum_{k=0}^{8}f_k^{eq} \quad (10a)$$

$$p=\rho c_s^2 \quad (10b)$$

$$\vec{u}=\frac{1}{\rho}\sum_{k=0}^{8}c_kf_k=\frac{1}{\rho}\sum_{k=0}^{8}c_kf_k^{eq} \quad (10c)$$

$$T=\sum_{k=0}^{8}g_k=\sum_{k=0}^{8}g_k^{eq} \quad (10d)$$

The time step size ($\delta t$) is same with lattice length ($\delta$), therefore, lattice speed (Eq. 6) is taken as an unity. Lattice sound speed (Eq. 5) is $1/\sqrt{3}$

Detailed presentation of boundary condition implementations is omitted here for conciseness; however, it is available in A.A. Mohammad's work [21]. In LBM, boundary conditions can be implemented via distribution functions for the momentum and the energy equations. Owing to the streaming step of the LBM, there are unknown and known distribution functions, and unknown distribution functions are established using known distribution functions to apply all boundary conditions. In the momentum equations, no-slip boundary conditions are enforced at walls using the bounce-back rule, with the physical boundaries of the solution domain aligned with lattice grid lines. For the energy equation, constant temperature and zero heat flux boundary conditions are applied according to the determined four cases (Table 1). The LBM formulations described above are implemented in-house LBM code via FORTRAN programming.

### 1.3. Validation

To validate our LBM code, we extensively employ the validated finite-volume-based commercial CFD code Ansys-Fluent [19]. The Boussinesq approximation is utilized in the reference calculation, similar to LBM. The QUICK scheme is employed to discretize all convective terms. For pressure-velocity coupling, the SIMPLEC algorithm is utilized. The default under-relaxation parameters are set at 1.0 for pressure, 0.7 for momentum, and 1.0 for energy, respectively. Convergence criteria include a threshold of $10^{-6}$ for continuity, $x$-velocity, and $y$-velocity. In the case of the energy equation, a residual value of $10^{-8}$ is employed.

Validation is employed for the case of VHVC at the highest Rayleigh number ($Ra=10^7$). The same mesh numbers (200 lattices/finite volumes in the $x$-direction and 200 lattices/finite volumes in the $y$-direction) are used; therefore, a total of 40000 lattices/finite volumes are used for validation. These mesh numbers support the stability of LBM. Since the used lattice numbers are suitable for LBM stability, a grid independence study is not conducted. The dimensionless temperature gradient distribution, Nusselt number, along the hot and cold walls is calculated using the numerical grid adjacent to the wall for LBM and FVM. Then, the Nusselt number for each wall is determined by integrating the Nusselt numbers over the wall and dividing by the wall length. Table 2 represents the Nusselt number comparison for the case of VHVC at $Ra=10^7$. The Nusselt number is computed for both the cold and hot walls. The differences between LBM and FVM are 0.64% and 0.72% for the cold wall and hot wall, respectively. These difference values are acceptable; therefore, we validate our LBM code.

**Table 2**. Nusselt number comparison for VHVC at $Ra=10^7$

| $Nu$ | LBM | FVM | Difference (%) |
|---|---|---|---|
| Cold wall | 17.8587 | 17.7434 | 0.64 |
| Hot wall | 18.0579 | 17.7345 | 2.40 |

### 2. Conclusions and Discussion

Figure 3 shows the nondimensional streamlines at the highest Rayleigh number ($Ra=10^7$). A total

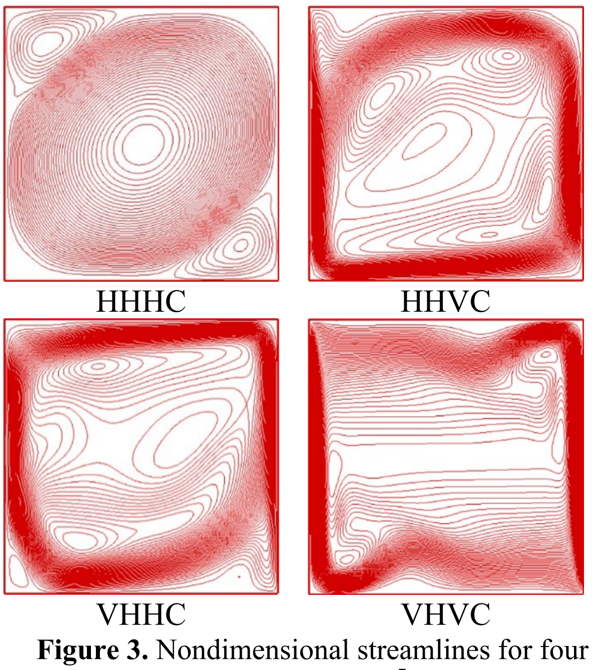


**Figure 3.** Nondimensional streamlines for four cases at $Ra=10^7$

of 51 streamlines are used in the all cases for better comparison, therefore step size between streamlines is 0.01960. In the symmetric cases, such as HHHC and VHVC, the streamlines exhibit greater symmetry. At lower Rayleigh number, which are not shown here, the degree of symmetry becomes even more evident. In

HHHC, the streamlines are less dense near the wall, whereas in the other cases, the streamlines near the wall are denser. Streamlines on heated and cooled surfaces exhibit higher density compared to adiabatic surfaces.

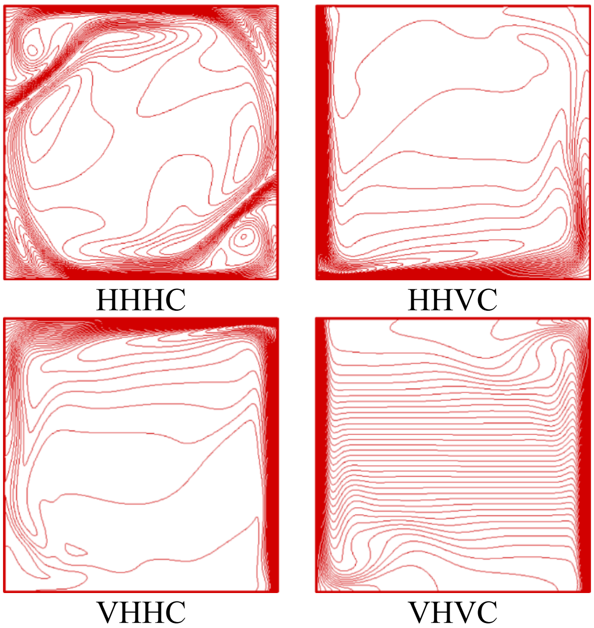


**Figure 4.** Isotherm for four cases at $Ra$=$10^7$

Isotherms are represented at the highest Rayleigh number ($Ra$=$10^7$) in Figure 4. Here, again a total 51 isotherms are used in the all cases for better comparison. The step size between isotherms is 0.01960. Streamlines characteristics effect the isotherms, therefore the same comments can be done for isotherms. In the symmetry cases, like HHHC and VHVC, the isotherms display greater symmetry. As we move to lower Rayleigh numbers, although not depicted here, the level of symmetry becomes even more pronounced. In the case of HHHC, the streamlines are less concentrated near the walls, whereas in other cases, the isotherms near the wall become denser. Isotherms on heated and cooled surfaces demonstrate a higher concentration when compared to adiabatic surfaces. Cases characterized by dense isothermals at the walls produce higher Nusselt numbers. Consequently, at Ra=$10^7$, VHVC yields the highest Nusselt number. Subsequently, cases of VHVC and HHHC produces equivalet Nusselt numbers. On the other hand, HHHC produces lowest Nusselt number.

Figure 5 exhibits the Nusselt number variation with Rayleigh numbers for (a) cold wall and (b) hot wall. The Rayleigh number is presented in Figure 5 on a logarithmic scale. Nusselt number increases with Rayleigh numbers as expected. At Ra=$10^7$, the Nusselt number interpretations based on isotherms contours align with Figure 5.

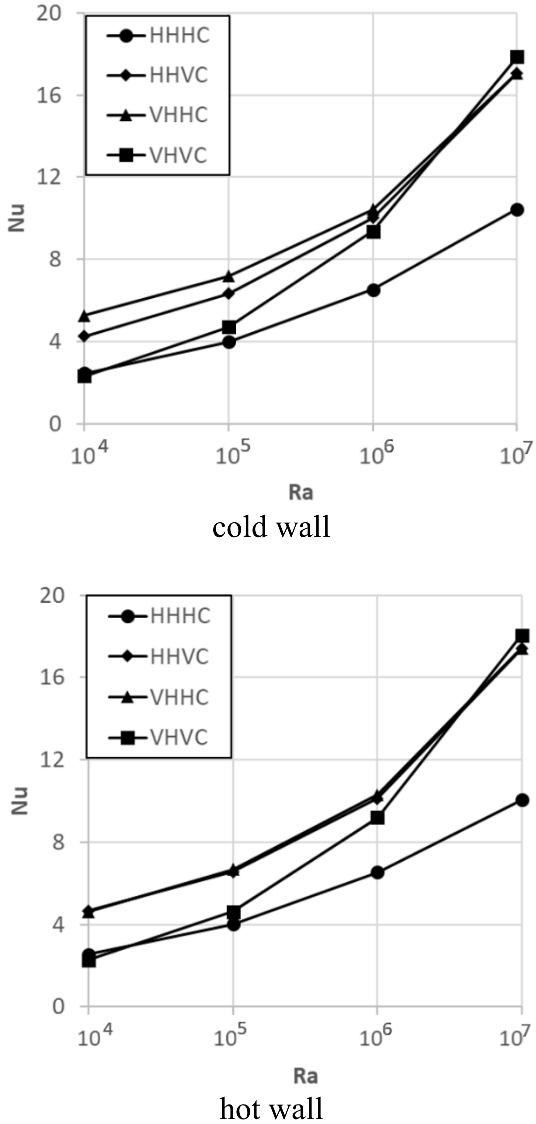


**Figure 5.** Nusselt number variation with Rayleigh numbers for (a) cold wall and (b) hot wall

In most cases, both cold and hot wall generally produced nearly equal Nusselt numbers, with exception occurring in nonsymmetric cases (HHVC and VHHC) for Rayleigh numbers of $10^4$, $10^5$ and $10^6$. At lowest Rayleigh number, HHHC and VHVC yields lowest Nusselt number. At the VHVC case, the Nusselt number increases rapidly with Rayleigh numbers, reaching its peak at the highest Rayleigh number.

Flow and heat characteristics are examined under four different cases and in laminar natural convection. The LBM requires more lattices due to stability issues at higher Rayleigh or Reynolds number. This is a limitation of the LBM. This study will involve turbulent flows, meaning it will work at higher Rayleigh numbers. For this purpose, turbulence model will be added or implemented to our in-house code.

## 3. Conclusion

In this paper, the lattice Boltzmann method (LBM) is utilized to model the cyclic natural convection phenomenon inside a square enclosure under laminar flow conditions. Various combinations of boundary conditions are applied to create different cases which are HHHC, HHVC, VHHC and VHVC. These cases are evaluated using four Rayleigh numbers ($Ra$=$10^4$, $10^5$, $10^6$, and $10^7$) to represent laminar flow conditions. In order to validate the results, the well-validated finite volume method-based commercial code, Ansys-Fluent, is employed [19]. Streamlines, isotherms and variation of Nusselt number with Rayleigh numbers are examined. The following conclusions can be obtained as below:

- Nusselt number increases with Rayleigh numbers.
- The characteristics of streamlines characteristics effect the isotherms, and since the isotherms are produced from nondimensional temperature contours, observations about the Nusselt number can be made by examining the isotherms.
- The case of HHHC has produces the lowest Nusselt number compared to the other cases.
- Symmetric cases (HHHC, VHVC) produce symmetric streamlines and isotherms, with the same manner, asymmetric cases (HHVC, VHHC) generate asymmetric streamlined and isotherms.
- At high Rayleigh numbers, the Nusselt numbers formed by the VHVC case are high, while at low Rayleigh numbers, the Nusselt numbers are low.
- Generally, asymmetric cases (HHVC, VHHC) produce same Nusselt numbers.
- The Nusselt numbers calculated from the cold wall and the hot wall are very close to each other especially at symmetry cases.

**Nomenclature**

| | |
|---|---|
| $c$ | lattice speed, [ms$^{-1}$] |
| $\vec{c}_k$ | discrete lattice velocity set, [ms$^{-1}$] |
| $c_s$ | lattice speed of sound, [ms$^{-1}$] |
| $c_p$ | isobaric spesicif heat, [Jkg$^{-1}$K$^{-1}$] |
| $F$ | External force (=$\rho g\beta[T - T_{mean}]$) |
| $f_k$ | discrete density distribution function, [kgm$^{-3}$] |
| $g$ | gravitational acceleration, [ms$^{-2}$] |
| $g_k$ | discrete temperature distribution function, [K] |
| $h$ | Convective heat transfer coefficient, [K] |
| $k$ | Thermal conductivity, [Wm$^{-1}$K$^{-1}$] |
| $L$ | length of domain, [m] |
| $Nu$ | Nusselt number (=$hL/k$) |
| $p$ | Pressure, [Pa] |
| $Pr$ | Prandtl number (=$\mu c_p/k$) |
| $Ra$ | Rayleigh number (=$g\beta\Delta T L^3/\nu\alpha$) |
| $q"$ | heat flux, [Wm$^{-2}$] |
| $T$ | temperature, [K] |
| $t$ | time, [s] |
| $\vec{u}$ | velocity vector |
| $W$ | width of domain, [m] |
| $w_k$ | weighting factors |
| $\vec{x}$ | position vector |
| $x, y$ | 2D Cartesian coordinates |
| | **Greek Symbol** |
| $\alpha$ | thermal diffusivity, [m$^2$s$^{-1}$] |
| $\beta$ | thermal expansion coefficient, [K$^{-1}$] |
| $\Delta T$ | temperature differences between hot and cold walls, [K] |
| $\delta$ | lattice unit (distance between to neighboring lattice nodes), [m] |
| $\delta_t$ | time step, [s] |
| $\theta$ | Nondimensonal temperature =$(T - T_F/T_W - T_F)$ |
| $\mu$ | dynamic viscosity, [kgms$^{-1}$] |
| $\nu$ | kinematic viscosity, [m$^2$s$^{-1}$] |
| $\rho$ | density, [kgm$^{-3}$] |
| $\omega$ | Collision for momentum transfer [s$^{-1}$] |
| $\omega_T$ | Collision for energy transfer [s$^{-1}$] |
| | **Acronyms** |
| HHHC | Horizontal hot horizontal cold |
| HHVC | Horizontal hot vertical cold |
| VHHC | Vertical hot horizontal cold |
| VHVC | Vertical hot vertical cold |

## Article Information Form

### *Authors Contribution*

Authors contributed equally to the study.

***The Declaration of Conflict of Interest/ Common Interest***

No conflict of interest or common interest has been declared by authors.

***The Declaration of Ethics Committee Approval***

This study does not require ethics committee permission or any special permission.

***The Declaration of Research and Publication Ethics***

Authors of the paper declare that they comply with the scientific, ethical and quotation rules of SAUJS in all processes of the paper and that they do not make any falsification on the data collected. In addition, they declare that Sakarya University Journal of Science and its editorial board have no responsibility for any ethical violations that may be encountered, and that this study has not been evaluated in any academic publication environment other than Sakarya University Journal of Science.

***Copyright Statement***



**References**

[1] G. De Vahl Davis, "Natural convection of air in a square cavity: A benchmark numerical solution," International Journal for Numerical Methods Fluids, vol. 3, pp. 249-264, May/June 1983.

[2] S. Ostrach, "Natural convection in enclosure," ASME Journal of Heat and Mass Transfer, vol. 110, pp. 1175-1190, 1988.

[3] J. L. Lage, A. Bejan, "The resonance of natural convection in an enclosure heated periodically from the side," International Journal of Heat and Mass Transfer, vol. 36, issue. 8, pp.2027-2038, 1993.

[4] M. Mahdavi, M. Sharifpur, H. Ghodsinezhad, J. P. Meyer, "Experimental and numerical study of the thermal and hydrodynamic characteristics of laminar natural convective flow inside a rectangular cavity with water, ethylene glycol-water and air," Experimental Thermal and Fluid Science, vol. 78, pp.50-64, 2016.

[5] N. Ugurbilek, Z. Sert, F. Selimefendigil, H. F. Oztop, "3D laminar natural convection in a cubical enclosure with gradually changing partitions," International Communications in Heat and Mass Transfer, vol. 133, 105932, 2022.

[6] T. Pesso, S. Piva, "Laminar natural convection in a square cavity: Low Prandtl numbers and large density differences," International Journal of Heat and Mass Transfer, vol. 53, issue. 3-4, pp. 1036-1043, 2009.

[7] M. Turkyilmazoglu, "Exponential nonuniform wall heating of a square cavity and natural convection," Chinese Journal of Physics, vol. 77, pp. 2122-2135, 2022.

[8] M. Turkyilmazoglu, "Driven flow motion by a dually moving lid of a square cavity," European Journal of Mechanics / B Fluids, vol. 94, pp. 17-29, 2022.

[9] Y. H. Qian, D. D'Humieres, P. Lalemand, "Lattice BGK models for Navier–Stokes equation," Europhysics Letters, vol. 17, issue.6, pp. 479-484, 1992.

[10] S. Y. Chen, G. D. Doolen, "Lattice Boltzmann method for fluid flows," Annual Reviews Fluid Mechanics, vol. 30, pp. 329-364, 1998.

[11] Y. H. Qian, S. Succi, S. A. Orszag, "Recent advance in lattice Boltzmann computing," Annual Reviews of Computational Physics III, pp. 195-242, 1995.

[12] C. K. Aidun, "Lattice-Boltzmann method for complex flows," Annual Reviews of Fluid Mechanics, vol. 42, pp. 439-472, 2010.

[13] L. Chen, Q. Kang, Y. Mu, Y. L. He, W. Q. Tao, "A critical review of the pseudopotential multiphase lattice

Boltzmann model: Methods and applications," International Journal of Heat and Mass Transfer, vol. 76, 210236, 2014.

[14] I. Taymaz, E. Aslan, A. C. Benim, "Numerical investigation of incompressible fluid flow and heat transfer across a bluff body in a channel flow," Thermal Science, vol. 19, issue. 2, pp. 537-547, 2015

[15] P. Karki, A. K. Yadav, D. A. Perumal, "Lattice Boltzmann computation of two dimensional differentially heated cavity of incompressible fluid with different aspect ratios," in International Conference on Intelligent Computing, Instrumentation and Control Technologies-2017, Kannur, Kerala, 2017, pp. 1540-1550.

[16] Y. Feng, S. Guo, W. Tao, P. Sagaut, "Regularized thermal lattice Boltzmann method for natural convection with large temperature differences," International Journal of Heat and Mass Transfer, vol. 125, pp. 1379-1391, 2018.

[17] Y. Wei, H. Yang, H. S. Dou, Z. Lin, Z. Wang, Y. Qian, "A novel two-dimensional coupled lattice Boltzmann model for thermal incompressible flows," Applied Mathematics and Computation, vol. 339, pp. 556-567, 2018.

[18] P. Pichandi, S. Anbalagan, "Natural convection heat transfer and fluid flow analysis in a 2D square enclosure with sinusoidal wave and different convection mechanism," International Journal of Numerical Methods for Heat & Fluid Flow, vol. 29, issue. 9, pp. 2158-2188, 2018.

[19] M. F. Hasan, M. M. Molla, S. Siddiqa, A. M. Khan, "Mesescopic CUDA 3D MRT-LBM simulaion of natural convection of poer-law fluids in a differentially heated cubic cavity with a machine learning cross-validation," Arabian Journal for Science and Engineering, vol. 49, pp 10687-10723, 2024.

[20] T. Li, C. Zhu, Z. Gao, P. Lei, S. Liu, "GPU parallel compuing based on PF-LBM method for simulation dendrites growth under natural convection condition," AIP Advances vol. 14, issue. 2, 025240, 2024.

[21] Ansys-Fluent, version 20.0, Canonsburf PA, Ansys-Inc, 2019

[22] P. L. Bahatnagar, E. P. Gross, M. Krook, "A Model for Collisional Processes in Gases I: Small Amplitude Processes in Charged and Neutral One-Component System," Physical Review, vol. 94, issue. 3, pp. 511-525, 1954.

[23] A. A. Mohamad, Lattice Boltzmann Fundamentals and Engineering Applications with Computer Codes. 2nd ed., London: Springer, 2019.